J Solid State Electrochem (2010) 14:811–816
DOI 10.1007/s10008-009-0856-8

ORIGINAL PAPER

Hybrid materials for supercapacitor application

A. Malak · K. Fic · G. Lota · C. Vix-Guterl · E. Frackowiak

Received: 25 March 2009 / Accepted: 24 April 2009 / Published online: 13 May 2009

Abstract In the present study, a manganese oxide obtained by the acid treatment of $LiMn_2O_4$ spinel has been used as a positive electrode of supercapacitor. Removal of lithium from a spinel allowed to obtain MnO_2 compound with the pores partly distributed in atomic scale, hence, an efficient use of its pseudocapacitive properties could be reached. On the other hand, residual lithium remaining in the structure preserved layered framework of MnO_2 with pathways for ions sorption. Physical properties, morphology, and specific surface area of electrode materials were studied by scanning and transmission electron microscopy, and nitrogen sorption measurements. Voltammetry cycling, galvanostatic charge/discharge, and impedance spectroscopy measurements performed in two- and three-electrode cells have been applied in order to measure electrochemical parameters. Neutral Li_2SO_4 aqueous solution has been selected for electrolytic medium. Extension of operating voltage for supercapacitor has been realized through asymmetric configuration with an activated carbon as a negative electrode. The asymmetric capacitor was operating within a voltage range up to 2.5 V (limited to 2.0 V for cycling tests) and was able to deliver a specific capacitance of 60 Fg^{-1} per capacitor at 100 mA g^{-1} current density. High specific energy of 36 Wh kg^{-1} was reached but with a moderate power density.

A. Malak · K. Fic · G. Lota · E. Frackowiak (✉)
Institute of Chemistry and Technical Electrochemistry,
Poznan University of Technology,
ul. Piotrowo 3,
60-695 Poznan, Poland
e-mail: Elzbieta.Frackowiak@put.poznan.pl

A. Malak · C. Vix-Guterl
Institut de Chimie des Surfaces et Interfaces (ICSI), CNRS,
15 rue Jean Starcky,
68057 Mulhouse, France

Keywords Manganese oxide · Pseudocapacitance · Asymmetric supercapacitor · Activated carbon

Introduction

Supercapacitors have attracted much attention because of their higher power density, better efficiency, and longer durability in comparison to the rechargeable batteries [1, 2]. Commercial devices are mainly based on two symmetric activated carbon electrodes and organic electrolyte, which has higher voltage stability than water medium. However, devices with organic electrolytes are ecologically unfriendly, less safe, and more expensive because of specific preparation conditions. Moreover, organic electrolytes have electrical conductivity ca. two orders of magnitude smaller than the aqueous medium; hence, it reduces available power, which is another serious drawback. It can be seen that using an aqueous electrolyte would be more interesting from an industrial point of view; but in an aqueous solution, despite of high specific capacitance, the cell voltage of symmetric devices is limited to 1 V, and subsequently, both power and energy densities remain unsatisfactory for industrial applications.

This fact led to the concept of asymmetric devices combining two different electrodes working in their optimal potential range: the negative one with high hydrogen overpotential and the positive one with high oxygen overpotential. It has already been proved that the cell voltage can be increased significantly with the use of hybrid system.

The reported example of such a system is a configuration using composite of manganese dioxide with multiwalled carbon nanotubes (MnO_2/MWNTs) as positive electrode and activated carbon as negative electrode. This combination allows to reach capacitance values up to 200 Fg^{-1}, and

it can additionally operate in a wide potential range (2 V in aqueous solution), increasing extremely energy of system [3, 4]. An increase of the operating voltage can be achieved due to a reversible hydrogen sorption in the pores of carbon material [5, 6].

Besides maximizing the operating voltage of a cell, capacitance of electrode is another matter which has to be considered in order to improve the performance of the supercapacitor. New trends are devoted to the application of materials with pseudocapacitance properties, which store energy through fast and reversible faradaic reactions, especially metal oxides and their composites with carbon materials [7–9].

Different transition metal oxides such as Co_3O_4, SnO_2, MnO_2, PbO_2, and V_2O_5 are being investigated as possible electrodes for electrochemical supercapacitors working in aqueous solution. According to literature data, various approaches have been attempted in order to synthesize transition metal oxides and their composites [7, 8]. These trials included electrodeposition or chemical synthesis of oxides with a porous morphology reduction of particle size, making composites with carbon nanotubes, carbon materials, conducting polymers, and mixed metal oxides; but the capacity of the materials is not significantly improved, indicating that the effective way for preparing metal oxide/carbon composites still needs to be found.

Some reports have been published about lithium-intercalated compounds such as $LiCoO_2$, $LiTi_5O_{12}$, or $LiTi_3O_7$ applied as electrodes in supercapacitors working in organic electrolyte [10, 11]. Also, a hybrid electrochemical supercapacitor with aqueous electrolyte and the activated carbon serving as a negative and $LiMn_2O_4$ as a positive electrode has been already investigated [12].

In our case, the enhancement of electrical properties has been achieved by immersing lithium manganese oxide powder in sulfuric acid in order to extract lithium ions from the intercalated compound. Mechanism of the removal of lithium from $LiMn_2O_4$ has been studied previously [13, 14], and the proposed reaction is as follows:

$$2Li\left(Mn^{3+}Mn^{4+}\right)O_4 + 4H^+ \rightarrow 3\lambda - MnO_2 + Mn^{2+}_{solution} + 2Li^+ + 2H_2O.$$

$LiMn_2O_4$ spinel has a cubic close-packed structure. Half of the octahedral sites of lattice are occupied by manganese ions and one-eighth of the tetrahedral sites by lithium ions. In stoichiometric spinel, the manganese ions coexist in two valence states, Mn^{3+} and Mn^{4+}, in equal proportions, hence, the chemical formula can be written as $Li(Mn^{3+}Mn^{4+})O_4$ [15]. It has been shown that treatment of the spinel-type material $LiMn_2O_4$ with aqueous acid leads to conversion of the $LiMn_2O_4$ to nearly pure MnO_2, while preserving the structural framework of the $LiMn_2O_4$ [13]. After treatment, most of the lithium ions are removed from the tetrahedral sites, but the structural framework of spinel is preserved. The final material is designated as λ-MnO_2. It was mentioned that the dissolution of manganese induced by acid treatment can also occur which results in oxidizing a part of Mn^{3+} ions to higher oxidation state Mn^{4+} [14, 16].

In this work, the physicochemical and electrochemical properties of the λ-MnO_2 prepared from lithium manganese oxide compound are presented. Partially lithiated λ-MnO_2 operating as a positive electrode has been successfully used for an asymmetric supercapacitor configuration. Additionally, this work promotes a system with aqueous electrolyte, which is cheaper and, what is more important, much more environmentally friendly.

Experimental

Materials preparation

Powder of lithium manganese oxide, $LiMn_2O_4$, was supplied by MERCK (lithium manganese (III, IV) oxide cathode powder, 180.81 g mol^{-1}). Sulfuric acid (95%), lithium sulfate, and potassium hydroxide were commercially available reagents (p.a.) from POCH and CHEMPUR. To prepare a carbon material for the negative electrode, a chemical KOH activation technique at 750°C temperature has been employed where the initial precursor material was biomass. The resulting activated carbon is denoted as SA.

Lithium extraction leading to the λ-MnO_2 compound was achieved by immersing the $LiMn_2O_4$ powder in 100 ml of 0.5, 1.0, and 5-mol L^{-1} sulfuric acid aqueous solution. Mixture was stirred for 2 h. After that, the solution was filtered, washed several times with distilled water, and dried in air at 100°C. The final product is designated λ-MnO_2.

Physical measurements

The specific surface area was determined by nitrogen sorption at 77 K (Brunauer, Emmett, and Teller method), and average pore size was estimated from the Barrett, Joyner, and Halenda method using Micromeritics ASAP 2010. The detailed texture and morphology observations of the samples were performed using a transmission electron microscopy (TEM) Philips CM200 and scanning electron microscopy (SEM) Philips 525.

Electrochemical characterization

The capacitor electrodes for evaluating the electrochemical properties were formed as pellets consisting of 75% composite material, 20% acetylene black, and 5% binder (polyvinylidene fluoride (PVDF), Kynar Flex 2801). In case of the asymmetric system, activated carbon SA (85%

active material, 10% PVDF, 5% acetylene black) was used as material of negative electrode. The typical mass of the positive electrode material was 11.0 mg and for negative, 12.5 mg. Supercapacitors were operating in 1 mol L^{-1} Li_2SO_4 electrolytic solution. All experiments were carried out at room temperature.

The capacitance values were estimated in two-electrode Swagelok® system by galvanostatic charge/discharge and cyclic voltammetry with different scan rates using VMP3 (Biologic–France). In the case of a three-electrode cell, Hg/Hg_2SO_4 system was used as a reference, however, the values of potential are expressed vs. normal hydrogen electrode (NHE). The capacitance values of material (either λ-MnO_2 or activated carbon) were calculated per mass of active material in one electrode. The specific capacitance has been evaluated using the formula $C=i\,\Delta t/(m\Delta V)$, where i is the current used for discharge, Δt is the time elapsed for the discharge, m is the mass of the active electrode, and ΔV is the voltage range of the discharge. In case of asymmetric system, all values were calculated for the total weight of the electrodes (including positive and negative one).

Results and discussion

Acid treatment of the spinel-type $LiMn_2O_4$ material leads to conversion of $LiMn_2O_4$ to MnO_2, while preserving the structural framework of the spinel (Fig. 1). After treatment, most of the lithium ions are removed from the tetrahedral sites, but the structural framework of the spinel is preserved because of the Li exchange with protons as well as the presence of residual lithium in the lattice. Replacing of lithium ions with protons that compensate charge is expected. Proposed mechanism for above-mentioned conversion involves diffusion of lithium from the structure in the analogical way to the proton diffusion during the reduction process of λ-MnO_2.

Figure 2 shows the texture of untreated $LiMn_2O_4$ (Fig. 2a) and acid treated λ–MnO_2 (Fig. 2b, c) where Fig. 2a, b show SEM and (Fig. 2c) TEM images. It is clearly seen that morphology of compound is greatly changed after a partial lithium removal; particles have more developed porosity, some irregularities are well visible at their surface. This suggests that the reaction may occur at the outer side of particles where lithium and also manganese ions can easily dissolve to the solution.

Manganese oxide partly lithiated has been used for electrochemical measurements. As it can be seen from Table 1, there was only a moderate difference in capacitance values between λ-MnO_2 obtained by sulfuric acid treatment with a concentration from 0.5 to 1 mol L^{-1} H_2SO_4. On the contrary, a significant decrease of capacitance occurs in the case of 5 mol L^{-1} H_2SO_4. It is assumed that acid with a higher concentration also easily dissolves manganese oxide framework. That is why for all the further investigations, λ-MnO_2 prepared from $LiMn_2O_4$ soaked in 1 mol L^{-1} sulfuric acid solution was chosen.

Specific surface area of material was determined to be 3.5 m^2g^{-1} for initial $LiMn_2O_4$ and 5 m^2g^{-1} for λ–MnO_2. The results from the nitrogen sorption isotherms proved that λ-MnO_2 is a mesoporous material with an average pore size of 35 nm. The meso/macroporosity has been also confirmed by SEM and TEM images.

Such negligible values of surface area indicate that capacitance of material cannot be ascribed to the electrostatic charge storage in the electric double layer, but faradaic reactions have to be involved. Calculated specific surface capacitance (capacitance expressed per surface area of λ-MnO_2) reaches a huge value of 4,200 μF cm^{-2}; whereas, typically, for carbon, it ranges from 10 to 20 μF cm^{-2}. On

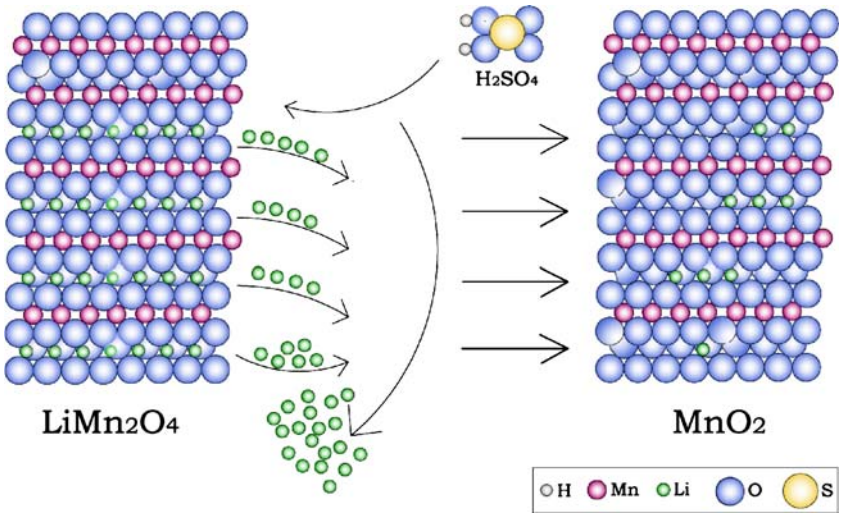

Fig. 1 General presentation of lithium removal from $LiMn_2O_4$ spinel

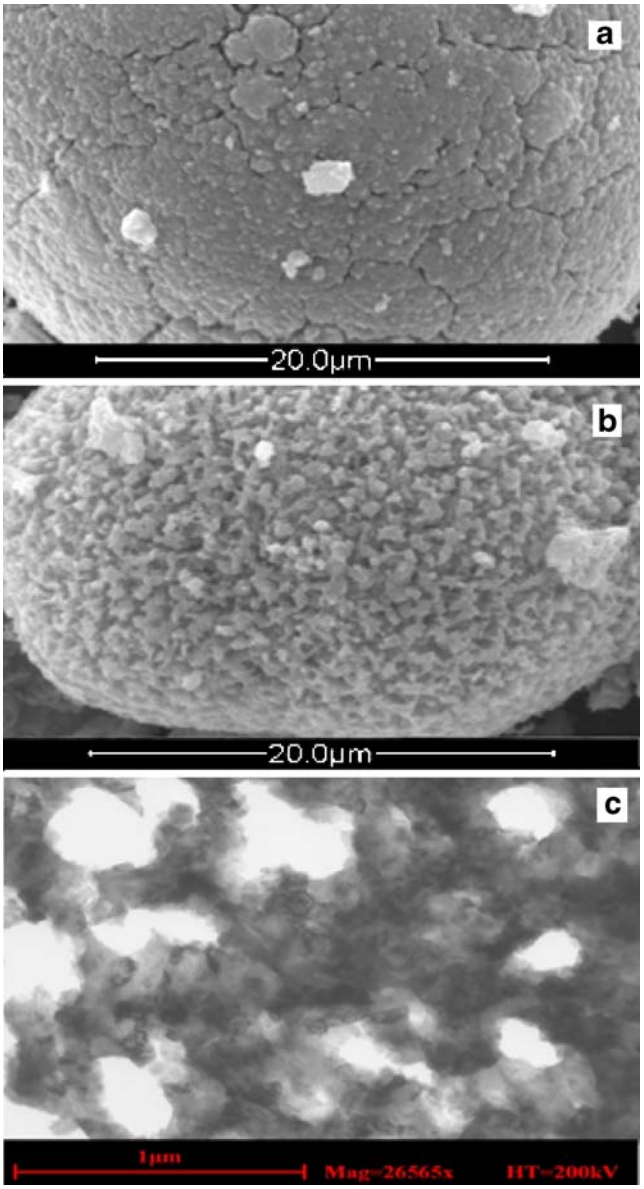

Fig. 2 SEM (**a**, **b**) and TEM (**c**) images of spinel (**a**) and manganese oxide (**b**, **c**)

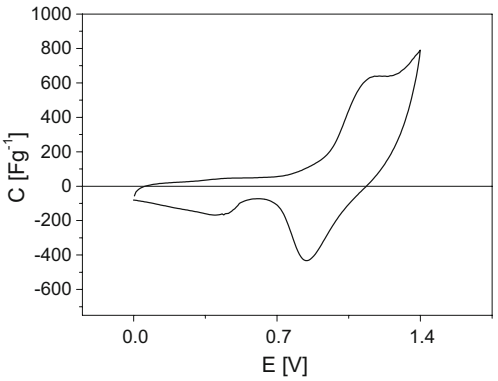

Fig. 3 Capacitance characteristics for the λ-MnO_2 electrode within potential range from 0 to 1.4 V vs. normal hydrogen electrode at a scan rate of 1 mV s^{-1} in 1 mol L^{-1} Li_2SO_4 solution

the other hand, specific surface area of carbon material used for negative electrode is equal to 898 m^2g^{-1} that gives specific surface capacitance of 16 μF cm^{-2}.

Figures 3 and 4 show cyclic voltammograms of λ-MnO_2 and activated carbon electrodes, respectively. Both electrodes were operating in 1 mol L^{-1} Li_2SO_4 aqueous solution but in the different range of potentials. λ-MnO_2 electrode was working within the potential window of 0.0–1.4 V vs. NHE. The cyclic voltammetry curve for this material does not have a rectangular shape, but due to the faradaic reactions, some well-defined peaks can be observed. Those peaks are related to the redox process of Mn with a simultaneous lithium ions insertion/deinsertion into the structure of λ-MnO_2 due to the fact that the structural framework of the initial spinel material is preserved. The potential values for these peaks well correlate with the thermodynamic Pourbaix data. For activated carbon, the potential range was from −1.0 to 0.4 V vs. NHE, and nearly rectangular shape of the registered curve can be observed. This indicates a typical electric double layer behavior; however, some redox reactions should not be excluded

Table 1 Capacitance values estimated at different current loads for manganese oxide obtained using different acid concentration

Acid [$molL^{-1}$]	Capacitance [F g^{-1}]			
	100 [mAg^{-1}]	200 [mAg^{-1}]	500 [mAg^{-1}]	1,000 [mAg^{-1}]
0.5	210	150	70	33
1.0	210	151	64	20
5.0	145	87	22	5

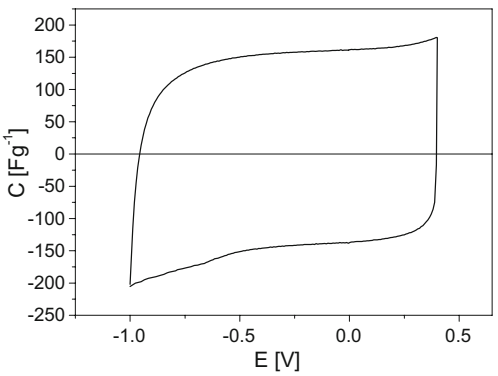

Fig. 4 Capacitor characteristics of the activated carbon electrode in potential range from −1.0 V to 0.4 V vs. normal hydrogen electrode at scan rate of 1 mVs^{-1} in 1 mol L^{-1} Li_2SO_4 solution

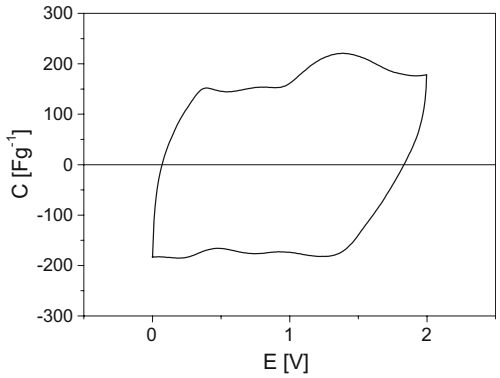

Fig. 5 Capacity characteristic of the asymmetric system (λ-MnO_2 material as a positive electrode combined with SA as negative one) at scan rate of 1 mV s^{-1} in 1 mol L^{-1} Li_2SO_4 aqueous solution

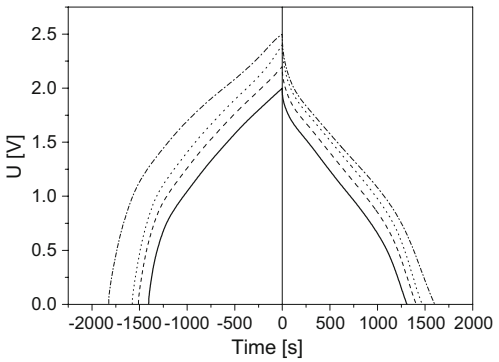

Fig. 7 Galvanostatic charge/discharge curves of asymmetric capacitor at a constant current density of 200 mA g^{-1} in 1 mol L^{-1} Li_2SO_4 aqueous solution

because the oxygen and nitrogen presence originated from biomass precursor.

Combination of λ-MnO_2 as positive and activated carbon as negative electrode led to the asymmetric capacitor being able to work within extended potential window. Figure 5 presents the capacitor characteristics of asymmetric system recorded at a scan rate of 1 mV s^{-1} up to 2 V vs. NHE. There is no oxygen and hydrogen evolution peaks on λ-MnO_2 and activated carbon respectively, which suggests that the electrolyte remains stable in this potential range.

Galvanostatic charge/discharge measurements at a different current density and within different voltage range were applied to estimate electrochemical properties such as values of specific capacitance, energy, and power. Investigations revealed that this capacitor is able to work within the potential range up to 2.5 V at a constant current of 200 mA g^{-1} and to 2.4 V for 100 mA g^{-1}. These results are shown in Figs. 6 and 7, respectively.

In the case of activated carbon serving as a negative electrode, the charge is stored electrostatically in the electrical double layer as well as by a reversible hydrogen storage mechanism. For the λ-MnO_2 electrode, faradaic reactions are involved in charging/discharging process with various oxidation state of manganese. This is the reason for a non-ideal shape of galvanostatic charging/discharging curves (convex shape of curves can be observed instead of triangle, especially for the lower values of constant current).

Influence of current density on the discharge time, in turn, on the specific capacitance, is shown in Fig. 8. As it can be seen from these charge/discharge curves, discharge time decreases with the increasing of the applied current, hence, the capacitance decreases. This is because the redox reactions depend on the insertion–deinsertion of the Li ions or protons from the electrolyte. At lower current densities, ions can penetrate into the inner-structure of the electrode material, having access to almost all available pores of the electrode, which leads to a complete insertion reaction and complete deinsertion afterwards; but at higher current densities, an effective utilization of pseudocapacitive material for the ion insertion is limited only to the outer surface of electrodes. It results in the reduction of specific capacitance values. The same phenomenon has been observed for increasing the voltage scan rate.

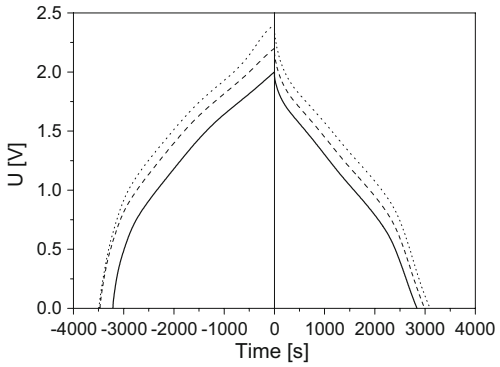

Fig. 6 Galvanostatic charge/discharge curves of asymmetric capacitor at a constant current density of 100 mA g^{-1} in 1 mol L^{-1} Li_2SO_4 solution

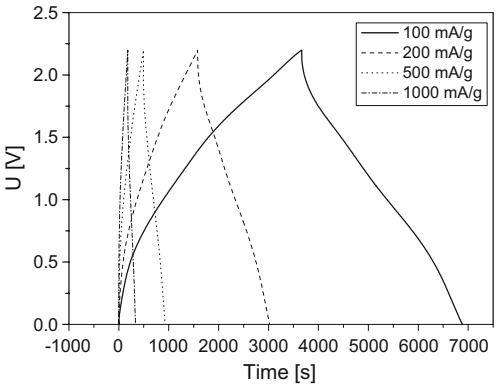

Fig. 8 Galvanostatic charge/discharge curves of asymmetric capacitor at different current densities in 1 mol L^{-1} Li_2SO_4 aqueous solution

As the scan rate increases, the cyclic voltammetry profile deviates from the ideal capacitive behavior. The main reason for such a behavior is that the higher sweep rate prevents the accessibility of ions to all the pores of the electrode. At high scan rates, a movement of ions is limited due to their slow diffusion, and only the outer surface can be utilized for charge storage. It has also been confirmed by electrochemical impedance spectra performed in the frequency range from 100 kHz to 1 mHz. Even if the equivalent series resistance was not very high, diffusion limitation are very pronounced.

The asymmetric supercapacitor characteristics at different current densities have been presented in the form of the Ragone plot. The specific energy density was calculated for the two electrodes (together with additives). Obviously, for the energy and power calculation, the voltage value without ohmic drop was taken. The high values of 36 Wh kg^{-1} have been obtained. However, the system could not supply a high power. The specific energy was 24 Wh kg^{-1} at 180 Wkg^{-1}. It is noteworthy that this novel manganese oxide material is still not yet optimized.

The trials have been undertaken for modeling of electrode/electrolyte interface and computer simulation of electrochemical characteristics. Artificial neural networks have been employed for determination and predicting charge/discharge characteristics during long-term cycling.

Conclusions

It has been proved that application of two different electrode materials operating in their optimal potential range allows to extend the working voltage of the whole capacitor system up to 2 V. Detailed analysis (theoretical and experimental) shows that MnO_2 electrode will operate in a more narrow range (ca. 0.8 V) of potential than carbon electrode.

The supercapacitor consisting of lithiated λ-MnO_2 material working as a positive electrode and activated carbon as negative one delivered a capacity of 60 Fg^{-1}, based on the total weight of both electrodes (positive and negative). It has been proved that an asymmetric configuration is superior in comparison to a symmetric one. Manganese oxide from spinel is a promising material but needs further improvement.

Acknowledgements The authors greatly acknowledge the financial support of the Ministry of Science and Higher Education (Poland) grant COST 31-1199/2007.

References

1. Burke A (2000) Ultracapacitors. Why, how and where is the technology. J Power Sources 91:37. doi:10.1016/S0378-7753(00)00485-7
2. Conway BE (1999) Electrochemical supercapacitors. Kluwer Academic, New York
3. Raymundo-Pinero E, Khomenko V, Frackowiak E, Béguin F (2005) Performance of manganese oxide/CNTs composites as electrode materials for electrochemical capacitors. J Electrochem Soc 152:A229. doi:10.1149/1.1834913
4. Khomenko V, Raymundo-Pinero E, Béguin F (2006) Optimisation of an asymmetric oxide/activated carbon capacitor working at 2 V in aqueous medium. J Power Sources 153:183. doi:10.1016/j.jpowsour.2005.03.210
5. Jurewicz K, Frackowiak E, Béguin F (2004) Towards the mechanism of electrochemical hydrogen storage in nanostructured carbon materials. Appl Phys A 78:981. doi:10.1007/s00339-003-2418-8
6. Béguin F, Friebe M, Jurewicz K, Vix-Guterl C, Dentzer J, Fracowiak E (2006) State of hydrogen electrochemically stored using nanoporous carbons as negative electrode materials in an aqueous medium. Carbon 44:2392. doi:10.1016/j.carbon.2006.05.025
7. Cottineau T, Toupin M, Delahaye T, Brousse T, Bélanger D (2006) Nanostructured transition metal oxides for aqueous hybrid electrochemical supercapacitors. Appl Phys A 82:599. doi:10.1007/s00339-005-3401-3
8. Huwe H, Fröba M (2007) Synthesis and characterization of transition metal and metal oxide nanoparticles inside mesoporous carbon CMK-3. Carbon 45:304. doi:10.1016/j.carbon.2006.09.021
9. Zhu S, Zhou H, Hibino M, Honma I, Ichihara M (2005) Synthesis of MnO_2 nanoparticles confined in ordered mesoporous carbon using sonochemical method. Adv Funct Mater 15:381. doi:10.1002/adfm.200400222
10. Du Pasquier A, Plitz I, Gural J, Menocal S, Amatucci G (2003) Characteristics and performacne of 500F asymmetric supercapacitor prototypes. J Power Sources 113:62. doi:10.1016/S0378-7753(02)00491-3
11. Du Pasquier A, Laforgue A, Simon P (2004) $Li_4Ti_5O_{12}$/poly (methyl) thiophene assymetric hybrid electrochemical device. J Power Sources 125:95. doi:10.1016/j.jpowsour.2003.07.015
12. Wang Y, Xia Y (2005) A new concept hybrid electrochemical supercapacitor: carbon/$LiMn_2O_4$ aqueous system. Electrochem Commun 7:1138. doi:10.1016/j.elecom.2005.08.017
13. Hunter JC (1981) Preparation of a new crystal form of manganese dioxide: λ-MnO_2. J Solid State Chem 39:142. doi:10.1016/0022-4596(81)90323-6
14. Ammundsen B, Aitchison PB, Burns GR, Jones DJ, Rozière J (1997) Proton insertion and lithium-proton exchange in spinel lithium manganates. Solid State Ion 97:269. doi:10.1016/S0167-2738(97)00065-9
15. Goodenough B, Manthiram A, Wnetrzewski B (1993) Electrodes for lithium batteries. J Power Sources 43:269. doi:10.1016/0378-7753(93)80124-8
16. Du Pasquier A, Blyr A, Courjal P, Larcher D, Amatucci G, Gérand B, Tarascon JM (1999) Mechanism for limited 55°C storage performance of $Li_{1.05}Mn_{1.95}O_4$ electrodes. J Electrochem Soc 146:428. doi:10.1149/1.1391625